WATER RESOURCES RESEARCH, VOL. 38, NO. 11, 1236, doi:10.1029/2001WR000746, 2002

Particle shape characterization using angle of repose measurements for predicting the effective permittivity and electrical conductivity of saturated granular media

Shmulik P. Friedman and David A. Robinson[1]

Institute of Soil, Water and Environmental Sciences, Agricultural Research Organization, Bet Dagan, Israel

Received 29 June 2001; revised 8 May 2002; accepted 8 May 2002; published 15 November 2002.

[1] The particle shape of sediments, soils, and rocks affects the packing of the material and the subsequent pore geometry; it therefore influences important transport properties, such as electrical conductivity, dielectric permittivity, diffusion coefficient, thermal conductivity, and hydraulic conductivity. It is difficult to quantify the ''average'' shape characteristics of a granular material so a method, which would capture the three-dimensional shape characteristics of a granular material in regards to its packing geometry, would be of great benefit. In this article we examine the use of the angle of repose and the maximum angle of stability of a slope of granular material poured into water, as a simple and rapid method of quantifying its ''effective'' particle shape. A two-stage concept is discussed relating the measured slope angles to the aspect ratio of an equivalent oblate ellipsoidal particle and using this aspect ratio for predicting the effective permittivity and bulk electrical conductivity of isotropic packings of granular materials. The slope angle-aspect ratio relationships were established using measurements of bulk electrical conductivity of monosized spherical glass beads and nonspherical sand and tuff grains packed in water to different porosities. This empirical relationship, the choice of an oblate geometry to represent particle shape, and a heuristic mixing model accounting for the effect of neighboring particles on the internal electrical field were tested using measurements of the effective permittivity for those granular media. Good agreement was found between the model predictions and measurements, indicating the physical significance of the above relationships and quantifiers. We have also tested and found high correlations between slope angles and a shape factor determined by image analysis of two-dimensional particle micrographs. We do not, however, propose to use it for routine particle shape characterization because of the insufficiently informative viewing of oblates from above and because of the expensive equipment and extensive work involve with it. Instead, we propose to use the easily measurable slope angles for routine particle shape characterization because of its simplicity and also because of its beneficial sensitivity to surface roughness and particle angularity effects beyond the aspect ratio of a smooth equivalent ellipsoid. *INDEX TERMS:* 1866 Hydrology: Soil moisture; 5109 Physical Properties of Rocks: Magnetic and electrical properties; 5139 Physical Properties of Rocks: Transport properties; *KEYWORDS:* particle shape, geometry, angle of repose, granular media, dielectric permittivity, electrical conductivity

Citation: Friedman, S. P., and D. A. Robinson, Particle shape characterization using angle of repose measurements for predicting the effective permittivity and electrical conductivity of saturated granular media, *Water Resour. Res.*, *38*(11), 1236, doi:10.1029/2001WR000746, 2002.

1. Introduction

[2] Particle shape plays a significant role in determining the magnitude of a number of physical properties of granular media. Electrical conductivity [*Fricke*, 1931; *Wyllie and Gregory*, 1953; *Meredith and Tobias*, 1962; *Zimmerman*, 1996; *Coelho et al.*, 1997], dielectric permittivity [*Sareni et al.*, 1997; *Sihvola*, 1999; *Jones and Friedman*, 2000], diffusivity [*Kim et al.*, 1987], thermal conductivity [*Torquato*, 1987] and hydraulic conductivity [*Wyllie and Gregory*, 1955; *Sperry and Peirce*, 1995; *Coelho et al.*, 1997] all depend on the shape and tortuosity of the pore network, which is itself largely dependent upon the shape of the grains constituting the matrix of a granular medium. Measured effective permittivity (ε_{eff}) is widely used to estimate the water content of rocks and soils [*Topp et al.*, 1980; *Sen et al.*, 1981; *Hallikainen et al.*, 1985; *Dirksen and Dasberg*, 1993; *Heimovaara*, 1993; *Kraszewski*, 1996]. The bulk (apparent) electrical conductivity (σ_a) is used to

[1]Now at U.S. Salinity Laboratory, Riverside, California, USA.

0043-1397/02/2001WR000746

estimate the solution conductivity in saline soils [*Rhoades et al.*, 1976; *Nadler and Frenkel*, 1980; *Mualem and Friedman*, 1991; *Rhoades et al.*, 1999] and the porosity of rocks [*Archie*, 1942; *Sen et al.*, 1981].

[3] Many models have been presented demonstrating the effect of particle shape on the electrical properties of granular materials [*Sihvola*, 1999, and references therein]. However, no single simple model has yet been demonstrated to work for porosities below 0.4 even for randomly packed spheres. Therefore, in this study we take a pragmatic approach to examine the effects of particle shape on electrical properties using a heuristic general mixing model proposed by *Sihvola and Kong* [1988]. In this model an adjustable parameter (a) accounts for the relative effect of neighboring particles on the internal electrical field of a given particle. This has the advantage of allowing us to fit the model to measurements with spheres as a reference, by adjusting the parameter, a. Using this determined parameter a, the depolarization factors in the model can be adjusted to reflect differing particle shapes. This allows us to explore the effects of particle shape on bulk electrical conductivity and effective permittivity.

2. Theoretical Considerations

2.1. Particle Shape Effect on Effective Permittivity and Electrical Conductivity

[4] The main objective of this study was to characterize the effective dielectric permittivity and bulk electrical conductivity based on some easily measured physical properties of granular materials. A model based on ellipsoidal particles provides convenient analytical expressions and great flexibility through alteration of the particle aspect ratio [*Landau and Lifshitz*, 1960]. By extending or contracting the b and c axes while keeping a constant a sphere can be transformed into either a disk-like (oblate) or needle-shaped (porlate) particle (Figure 1), representing many shapes encountered in the natural environment.

[5] The model presented by *Sihvola and Kong* [1988] describes a 2-phase isotropic medium, applicable to air-dried or water-saturated granular media. Their model contains a heuristic parameter, a, which varies from 0 to 1. The model is equivalent to the *Maxwell-Garnett* [1904] formula when the value of a is 0, the symmetric effective medium approximation [*Polder and van Santen*, 1946] for $a = 1 - N^i$ (2/3 for spheres), and the coherent potential formula [*Tsang et al.*, 1985] when a is 1. The Maxwell Garnett (a = 0) and coherent potential (a = 1) formulas constitute upper and lower bounds for the case of a better conducting background ($\varepsilon_0 > \varepsilon_1$). The model provides an implicit equation for calculating the effective permittivity (ε_{eff}) for non zero values of a:

$$\varepsilon_{eff} = \varepsilon_0 + \frac{\sum_{i=a,b,c} \frac{f(\varepsilon_1 - \varepsilon_0)\left[\varepsilon_0 + a\left(\varepsilon_{eff} - \varepsilon_0\right)\right]}{3\left[\varepsilon_0 + a\left(\varepsilon_{eff} - \varepsilon_0\right) + N^i(\varepsilon_1 - \varepsilon_0)\right]}}{1 - \sum_{i=a,b,c} \frac{fN^i(\varepsilon_1 - \varepsilon_0)}{3\left[\varepsilon_0 + a\left(\varepsilon_{eff} - \varepsilon_0\right) + N^i(\varepsilon_1 - \varepsilon_0)\right]}} \quad (1)$$

where the background permittivity is ε_0 and the permittivity of the inclusions with volumetric fraction f is ε_1. The depolarization factors (N^i) describe the extent to which the inclusion polarization is reduced according to its shape and orientation with respect to the applied electrical field. For an ellipsoid of revolution (spheroid, $a \neq b = c$) with an aspect ratio of a/b the depolarization factor can be approximated by (Figure 1) [*Jones and Friedman*, 2000]:

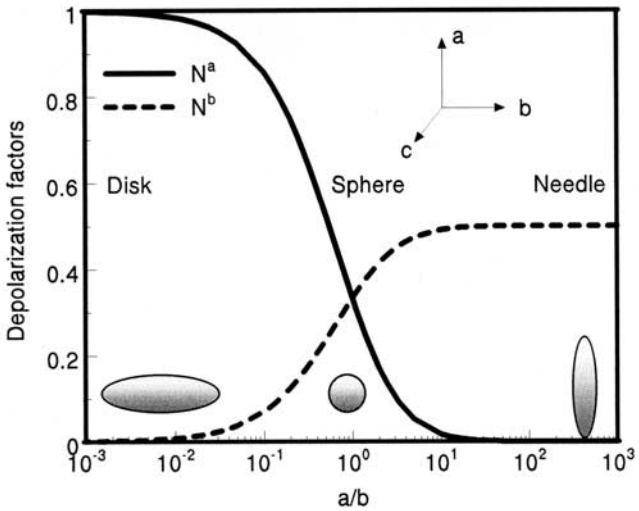

Figure 1. Depolarization factors of spheroids ($a \neq b = c$) as a function of aspect ratio, a/b.

$$N^a = \frac{1}{1 + 1.6(a/b) + 0.4(a/b)^2} \quad ; \quad N^b = N^c = 0.5(1 - N^a) \quad (2)$$

The depolarization factors for a sphere are $N^{a,b,c}$ = 1/3, 1/3, 1/3; for a thin disk (extreme oblate) $N^{a,b,c}$ are 1,0,0, and for a long needle (extreme prolate) $N^{a,b,c}$ are 0, 1/2, 1/2.

[6] Bulk electrical conductivity, σ_a, of water-saturated, coarse-textured media with negligible surface conductivity presents a similar physical problem. Therefore the same equation (1) is used, with the value of ε_0 replaced by the electrical conductivity of the solution, σ_w, and the value of ε_1 replaced by the electrical conductivity of the matrix, σ_s. Most natural minerals are not conducting (e.g. $\sigma_s < 10^{-10}$ S m^{-1} for quartz). Therefore, while the effective permittivity is a finite contrast ($\varepsilon_0/\varepsilon_1$) conductivity problem [*Jones and Friedman*, 2000], the σ_a/σ_w can be regarded as a 1/0 (σ_w/σ_s) conductivity problem for the same geometry [*Friedman and Jones*, 2001].

[7] Simple analytical expressions exist for the bulk transport properties of mixtures of ellipsoids, e.g. Equation 1, but at present, there is no way of linking an "equivalent" ellipsoid to simple measurements performed on the actual nonellipsoidal particles. An "equivalent" ellipsoid would have to be used as real grains do not strictly conform to ellipsoids. However, it is feasible that the equivalent ellipsoid geometry will posses the same predictive behavior in terms of physical processes as the granular material it endeavors to describe.

2.2. Methods of Characterizing Particle Shape

[8] Experimentalists and modelers have developed different approaches to characterize particle shape. An attempt to quantify the shape of grains was proposed by *Wardell* [1935]. He placed particles under a microscope and photographed their plan image to give a two-dimensional view of the maximum cross section. Gravitational forces will gen-

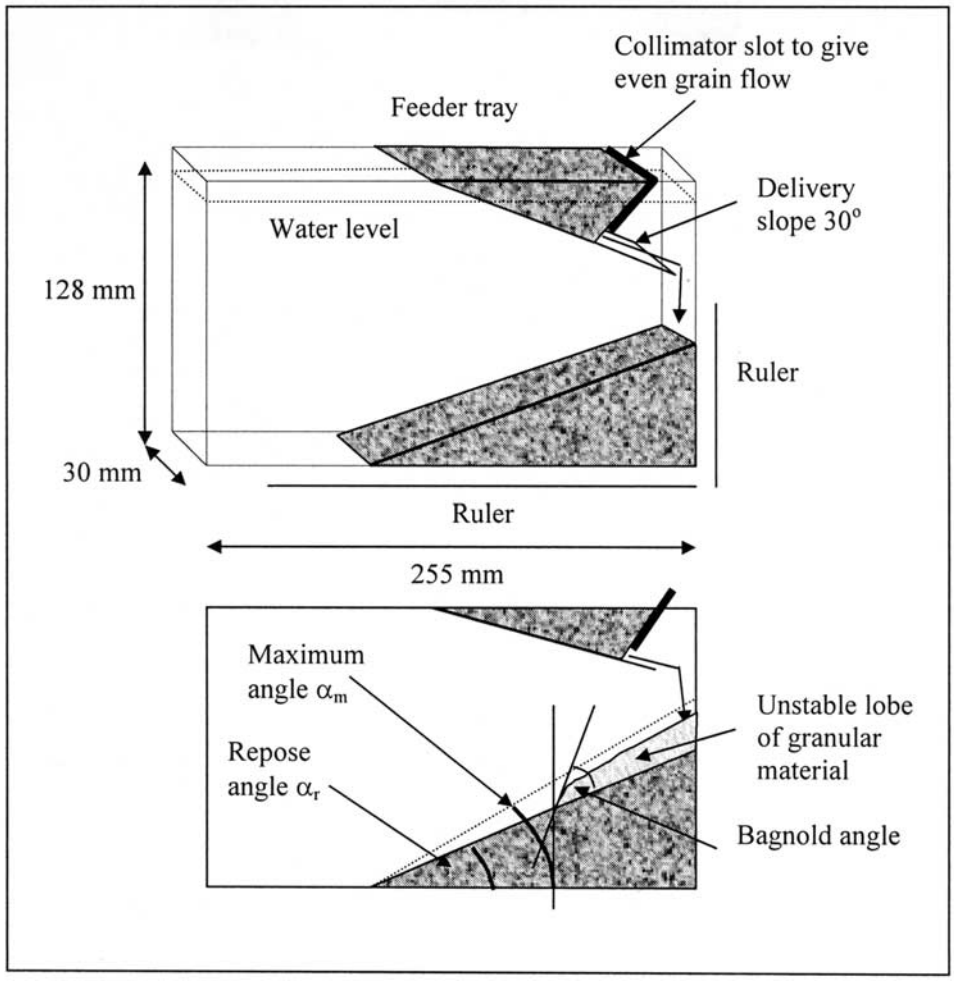

Figure 2. Schematic diagram of the Hele-Shaw cell used to measure the slope angles. The lower diagram shows the maximum and minimum angles measured.

erally ensure that the view is close to the maximum possible projected area. The area of this image of the grain (A_p) is then compared with the area of the smallest inscribed circle into which the grain fits in its entirety (A_c). In *Wardell*'s [1935] discussion of shape, the ratio of the areas is defined as the sphericity (S):

$$S = \frac{A_p}{A_c} \tag{3}$$

An alternative shape factor (S_f) used in many image analysis programs (e.g., Sigma Scan Pro5, SPSS Science, Chicago, Illinois) is defined as:

$$S_f = \frac{4\pi A_p}{P^2} \tag{4}$$

where P is the length of the perimeter of the particle. Both ratios are 1 for spheres and decline as the grains become less spherical. This definition of "shape factor", used here, is termed differently by other authors, e.g. circularity [*Podczeck*, 1997] and 1/roundness [*Brown and Vickers*, 1998]. (It is different from the 3-D shape factor, S_F, of Figure 8 of *Jones and Friedman* [2000].) The shape factor, S_f, has the advantage of also incorporating a measure of the roughness of the particle, which Wardell's sphericity does not. However, the quality of the determination of the perimeter and area depends on photograph quality and resolution. This is especially significant for particles with fractal surfaces for which S_f should, in principle, approach zero.

[9] When dealing with granular materials of close to spherical particles rather than platy or needle-like materials it is sensible to assume that the 2-dimensional projected image is a reliable approximation of the 3-dimensional particle, namely, that the projected cross-section and the one orthogonal to it are statistically similar. This is not the case for nonspherical (ellipsoidal) particles. If the particles are prolate ($a > b = c$), then the smallest horizontal dimension (b) and height (c) of the particle will be approximately the same and a 2-D image should be enough to characterize the aspect ratio (a/b) of the particles. If on the other hand the particles are oblate ($a < b = c$), then the projected image will be of the b-c plane and further independent evaluation of the height (a) of the particle is required in order to characterize its shape. Ongoing studies involving the determination of the 3-D shape from a 2-D projection [*Vickers*, 1996; *Podczeck*, 1997; *Brown and Vickers*, 1998; *Vickers and Brown*, 2001] may improve particle shape characterization by photographing methods, but at present the information retrieved from a single 2-D projection is quite limited when concerning a particle of

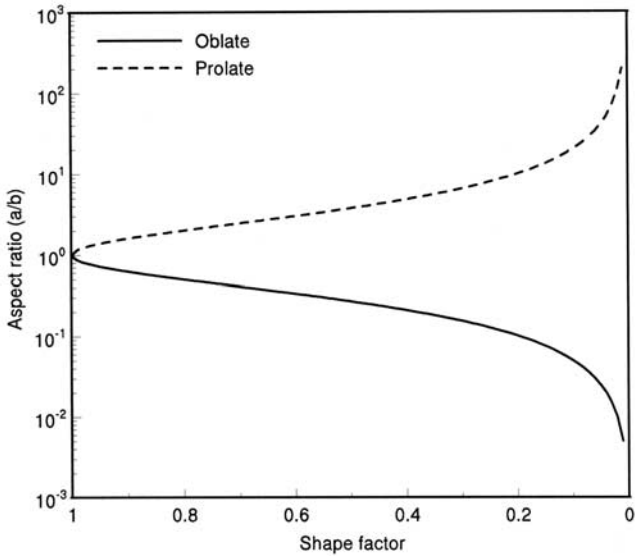

Figure 3. Relationship between ellipsoid shape factor ($4\pi A_p/P^2$) and aspect ratio (equation 6).

even idealized ellipsoidal shape. Other disadvantages of photographic methods are the expensive equipment required and the time consuming nature of the procedure, requiring 25 or more measurements on single grains to provide a statistically valid shape value for each granular material.

2.3. Slope Angle, Shape Factor, and Aspect Ratio

[10] It is well documented that the angle of repose of a dry granular material is related to the shape and roughness of the particles [*Yong and Warkentin*, 1975]. Granular media forming a pile are characterized by 3 angles [*Mehta*, 1994], described in Figure 2: The maximum angle of stability α_m, which is the angle of a slope prior to avalanching, the angle of repose, α_r which is the slope angle after avalanching and the Bagnold angle, Δ, which indicates the local deviation from the angle of repose. The maximum angle of stability has been of interest in the mechanics of granular media since *Coulomb* [1773] related it to the coefficient of internal friction, $\mu_s = \tan \alpha_m$. Rather than predicting the mechanical behavior of granular media, we are interested here in quantifying the effects of particle shape and surface roughness of a granular material on its effective permittivity and electrical conductivity. Since both the shape and the surface roughness affect these transport properties (ε_{eff} and σ_a), it is important that any characterization method can incorporate both features. A quick, inexpensive, simple method of characterizing the three-dimensional nature of grain shape and the way in which it configures itself during packing is therefore of some interest.

[11] *Sperry and Peirce* [1995] suggested using the slope angle of a poured granular pile as a way of quantifying the geometry of a granular medium. The method they used involved pouring a known mass of dry material into an empty Hele-Shaw cell and measuring the angle once all the material was deposited. One disadvantage of this method is that the angle measured lies somewhere between the angle of repose and the maximum angle of stability and the measurement is not repeatable. A refined method determining both the maximum and repose angles in a water-filled Hele-Shaw cell is proposed in this article.

[12] Using expressions for the perimeter, $2\pi\sqrt{0.5(a^2 + b^2)}$, and area, πab, of the projected ellipse of the *a*-*b* plane and the shape factor definition (equation 4), the aspect ratio and shape factor can be linked by

$$S_f = \frac{2(a/b)}{1 + (a/b)^2} \tag{5}$$

and

$$a/b = \frac{S_f}{1 \pm \sqrt{1 - S_f^2}} \tag{6}$$

where the positive sign is for oblate and the negative for prolate particles (Figure 3). Potentially therefore the angle of repose can be linked with a shape factor directly related to an aspect ratio of an equivalent ellipsoid, providing an easily measured parameter that can be used for predicting the effective permittivity and bulk electrical conductivity–porosity relationships ($\sigma_a(\phi)$ and $\varepsilon_{eff}(\phi)$).

3. Materials and Methods

3.1. Granular Materials and Photographic Image Analysis

[13] Three granular materials were used in this study, glass beads (Mo-Sci Corp., Rolla, MO, USA), quartz grains (Yerucham Crater, Negev desert, Israel) and tuff grains (Ramat Ha-golan, Israel). All materials were rinsed in deionized water. The quartz grains were first acid-washed to remove oxide coatings. The particles were all sieved to separate them into particle size classes, which are provided with some other physical characteristics in Table 1. The tuff particles do not contain significant internal porosity as indicated by their high particle density (ρ_s = 2.88 g/cm^3); the high porosities of their packings (0.60 to 0.63) stem from their angular shapes and rough surfaces. Photographs of the three materials are presented in Figure 4. The shape factors for these materials were determined by digitally photographing (Aplitac Lis 700 camera) 30 particles under a microscope (Olympus BX60) at 40× magnification. The 2-D projected images of the glass beads were not circular but elliptical with an aspect ratio of 1.10. We used the glass beads as reference spheres and contracted all the images by a factor of 1/1.10 to correct/calibrate the optics of the system. The corrected digital images with each pixel repre-

Table 1. Physical Characteristics of the Materials Used in the Study

	Glass Beads	Quartz Grains	Tuff Grains
Particle density, g cm^{-3}	2.48	2.65	2.88
Particle size classes, μm			
Large	425–500	425–500	425–500
Medium	180–200		
Small	90–106		
Very small	45–51		
Porosity range	0.36–0.41	0.34–0.44	0.60–0.63
Sphericity S[a]	1.00	0.73 (±0.09)	0.59 (±0.10)
Shape factor S_f[b]	1.00	0.78 (±0.04)	0.60 (±0.08)
Solid permittivity ε_s	7.6	4.7	6.0

[a] Equation 3.
[b] Equation 4.

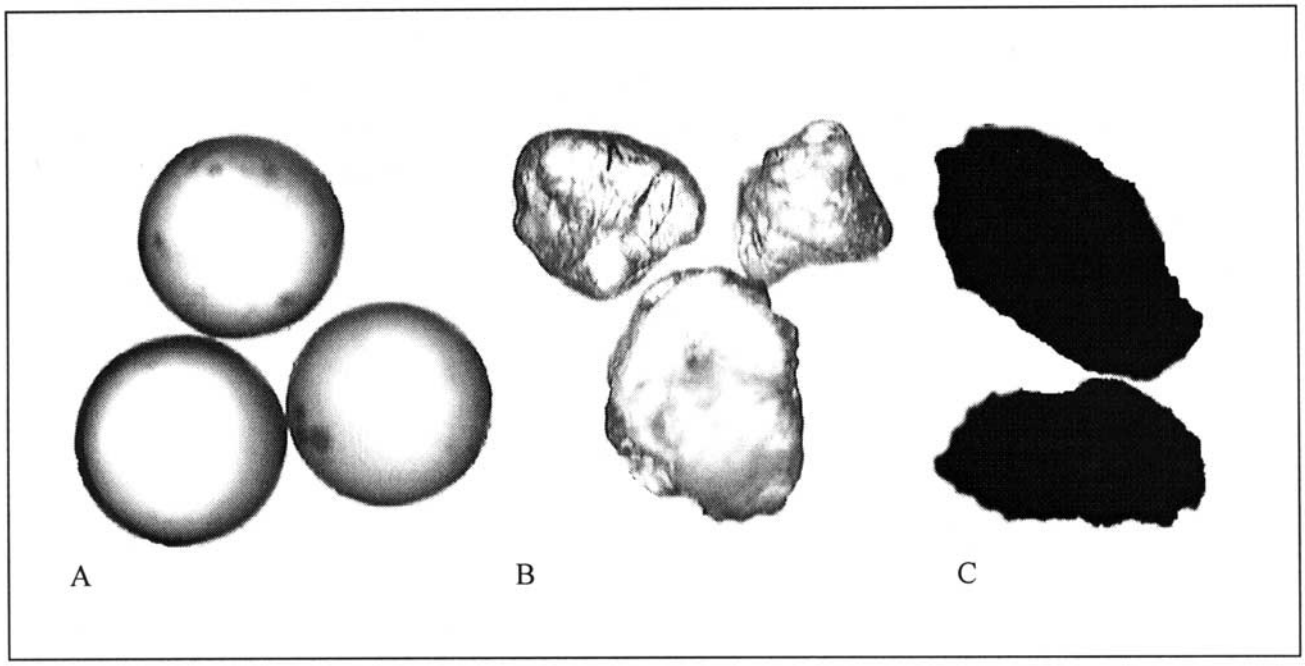

Figure 4. Microscope photographs of (a) glass beads, (b) sand grains, and (c) tuff grains. All grains approximately 500 μm in diameter.

senting 2.3 μm were then analyzed to determine the shape factor (S_f) and sphericity (S) using the Sigma Scan Pro5 image analysis software (SPSS Science, Chicago, IL).

3.2. Cell Design and Slope Angle Measurements

[14] A Hele-Shaw cell was constructed from Plexiglas to obtain the measurements of both the angle of repose and the maximum angle of stability while pouring grains from a wedge-shaped pile formed on a ramp (Figure 2). An even distribution of grains across this delivery slope and a controlled application rate was achieved using a "collimator" slot to regulate the flow. The aperture size was adjusted to a suitable position so that flow rates were about 0.4 g s^{-1}. The dimensions of the cell are important as the sidewalls can interact with the grains. Work presented by *Koeppe et al.* [1998] for binary mixtures of sugar and sand grains, for example, demonstrated that the mixing and segregation of material within a Hele-Shaw cell depends on both the separation of the sidewalls and the flow rate of the granular media into the cell. They found surprisingly that at certain flow rates and sidewall separations the media would segregate and form stratified layers within the slope. Based on these findings a spacing of 30 mm was chosen for our apparatus to minimize interaction with the sidewalls.

[15] The construction of the Plexiglas Hele-Shaw cell was straightforward. However, initial experimental results conducted with dry media, highlighted several problems. The Plexiglas created a static electric charge that affected the flow of the dry grains and even the use of an anti-static spray could not satisfactorily overcome this. More importantly it was found that the momentum of the grains falling onto the pile obliterated the top of the slope making the slope angle difficult to measure accurately. Reducing the flow rate of the grains to reduce the momentum transfer by reducing the collimator slot aperture caused clogging (with the larger grains) and an uneven flow of grains. To overcome these problems, we conducted the experiments under water, as we anticipated that the density of the fluid would increase the buoyancy of the grains, therefore reducing their speed and momentum transfer. This approach also removed the problem of static binding and reduced the friction between the grains and the collimator aperture, giving an even flow. The use of water allowed for the formation of a well-defined slope and was found to work well for particle sizes between 100 and 500 μm. However, particles less than 100 μm were influenced by the currents set up in the cell

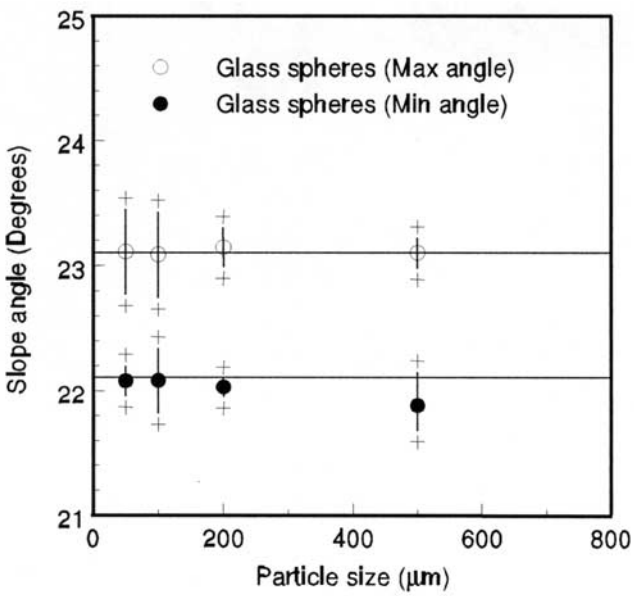

Figure 5. Slope angles as a function of particle size for glass spheres. The crosses represent 1 standard deviation. Particle sizes 100, 200, and 500 μm were measured under water where as 50 μm was measured in air.

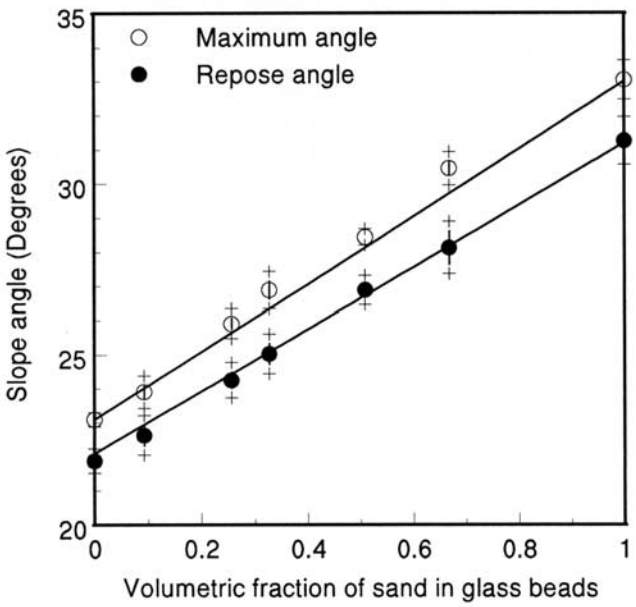

Figure 6. Slope angles as a function of the volumetric fraction of sand grains mixed into glass spheres. The crosses represent 1 standard deviation. The lines are the prediction based on the arithmetic mean of its components (equation 7).

caused by the flow of the grains. This procedure therefore is not suitable for materials less than 100 μm in diameter.

[16] The measurements of the documented maximum and repose angles started once a periodical steady state of accumulation and collapse was reached. In general, measurements were taken once a slope had reached at least 50 mm in length, and stopped after 10 sets of angle determinations. The height could be measured to ±0.5 mm keeping the maximum error in the measurement of the slope angle to ±0.5°. As the slope became longer this error reduced.

3.3. Electrical Measurements

[17] Measurement of the effective permittivity was made using a Tektronix (1502C) TDR cable tester. The time domain reflectometer (TDR) was connected to a PC, which was used to collect and analyze waveforms using software developed by *Heimovaara and de Water* [1993]. The TDR was connected via a 1.8 m, (50-ohm RG 58) coaxial cable to a 200 mm long coaxial measurement cell, consisting of a steel pipe with an internal diameter of 26.5 mm and a 6 mm diameter cylindrical steel inner electrode. The coaxial cell was calibrated for effective length using deionized water in a similar manner to *Heimovaara* [1993]. The bulk electrical conductivity was measured using the same coaxial cell connected to a CDM 83 conductivity meter (Radiometer, Copenhagen).

4. Results and Discussion

4.1. Slope Angles and Particle Size

[18] Initially we examined the dependence of the maximum and repose angles on grain size within the size range of between 50 to 500 μm. Spherical glass beads with diameters of 50, 100, 200 and 500 were used to examine slope angles for monosize materials of the same shape (Table 1). The 50 μm measurements were carried out in dry air (relative humidity <40%) because, as discussed above, circulation currents prevented the formation of a measurable slope under water. The results of these measurements (Figure 5) suggest that the size of particles within the limits considered does not affect the maximum or repose angles (all reported angles here and below are the average of 10 sequential avalanches). This is in agreement with work presented by *Jaeger et al.* [1989]. The measured maximum angle of stability, 23.1 ± 0.4°, is in very good agreement with the theoretically predicted value of 23.4°, resulting from a simple calculation evaluating the maximum allowed base angle before the top particle rolls off a pyramid made of four frictionless spherical particles [*Barabási et al.*, 1999]. The same slope angles found for the glass beads in air (50 μm) and in water (Figure 5) also indicate that α_m and α_r are independent of the background fluid.

4.2. Slope Angles of Glass-Sand Mixtures

[19] A second set of measurements of maximum and repose angles was conducted using mixtures of sand grains and glass beads. Seven mixtures were tested with volumetric fractions of sand of 0, 0.09, 0.26, 0.33, 0.51, 0.66 and 1. The results are presented in Figure 6 along with lines representing the volumetric fraction weighted arithmetic mean of the component slope angles:

$$\alpha_{(\text{Mixture})} = \sum_i f_i \alpha_i \qquad (7)$$

where f_i is the volumetric fraction of a certain shape and α_i is its slope angle. The good fit between the data and

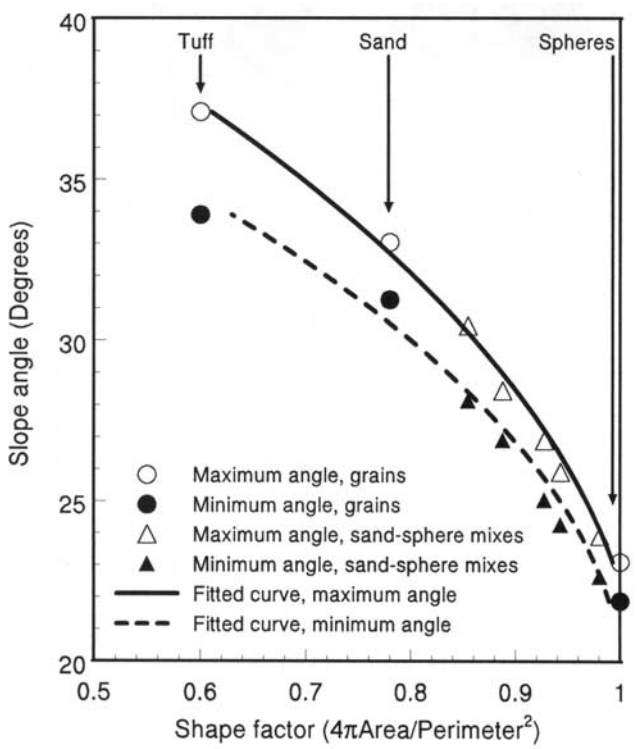

Figure 7. Slope angles as a function of the 2-dimensional imaged shape factor. The data for mixtures represent sand of volumetric fraction 0.09, 0.26, 0.33, 0.51, 0.67 mixed in glass spheres.

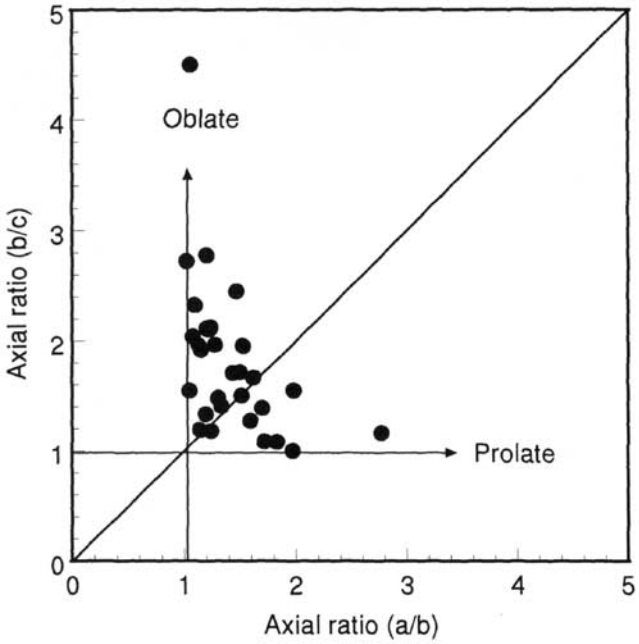

Figure 8. Axis ratios for tuff grains determined by three axial lengths measurements made with a micrometer.

the predicted response suggests that this simple fractional mixing formula is adequate over this range of slope angles.

4.3. Slope Angles and Photographically Determined Shape Factor

[20] The main objective of the present study was to propose the determination of maximum and repose angles as a method for characterizing particle shape, in terms of the aspect ratio of an equivalent oblate ellipsoid, for purposes of predicting the $\sigma_a(\phi)$ and $\varepsilon_{eff}(\phi)$ relationships. As an intermediate step, we consolidated the simple slope angles method by relating the measured angles to a standard, laborious, photographically determined, particle shape quantifier. Measured slope angles and shape factors determined from the 2-D projected image are presented in Figure 7. The high correlations are quite impressive. However, as discussed above, the 2-D projected image characterization can be considered reliable for only prolate particles. The relatively low aspect ratio of the tuff particles (a/b = 0.33) determined from the 2-D images suggests that they have a prolate shape. However, an independent measure of the height using a micrometer demonstrated that the particles tend toward oblates slightly more than toward prolates (Figure 8). This is one reason why in this work we take a pragmatic approach linking slope angles directly with aspect ratio of an equivalent oblate ellipsoid. For isotropic water-saturated packings, oblate particles make lower $\sigma_a(\phi)$ and $\varepsilon_{eff}(\phi)$ than do prolate particles of the same aspect ratio (a/b) [*Jones and Friedman*, 2000]. An additional reason for choosing an oblate particle shape for the sand and tuff grains was to incorporate surface roughness and particle angularity effects, which exist with real particles and are not taken into account by the aspect ratio of smooth ellipsoids.

4.4. Apparent Oblate Ellipsoid Determined From Electrical Conductivity Measurements

[21] The bulk electrical conductivity of packings of different grains was measured to determine the relationship between σ_a/σ_w and porosity ($\phi = 1 - f$). Using electrical conductivity is convenient as all the different grains were electrical isolators and therefore only differed in shape, unlike the dielectric problem where the grains have different solid permittivity values (Table 1). Results are presented in Figure 9 for glass spheres, quartz sand and tuff. Mixtures of quartz sand with glass spheres are bounded by the $\sigma_a/\sigma_w(\phi)$ relationship of each component taken separately, with successively lower conductivities as the mixtures increase in the quantity of nonspherical sand grains. Equation 1 written for electrical conductivity (interchanging $\varepsilon_{eff} \leftrightarrow \sigma_a$, $\varepsilon_0 \leftrightarrow \sigma_w$, and $\varepsilon_1 \leftrightarrow \sigma_s$, and letting $N^i = 1/3$ and $a = 0$) reduces to the well-known *Maxwell* [1954] equation:

$$\frac{\sigma_a - \sigma_w}{\sigma_a + 2\sigma_w} = f\frac{\sigma_s - \sigma_w}{\sigma_s + 2\sigma_w} \tag{8a}$$

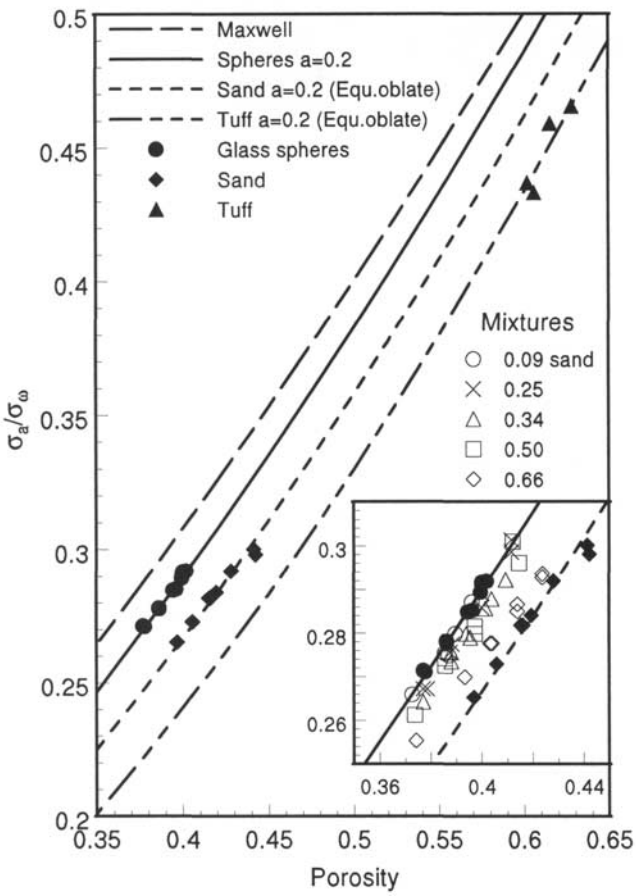

Figure 9. Ratio of the apparent electrical conductivity to that of the solution as a function of the porosity. Lines represent equation 1, the value of a fitted to the glass spheres data is 0.2. The main graph shows the glass beads, sand (a/b = 0.460), and tuff (0.350) grains, where the aspect ratios have been adjusted to fit the data. The inset graph shows data for sand mixed in glass beads.

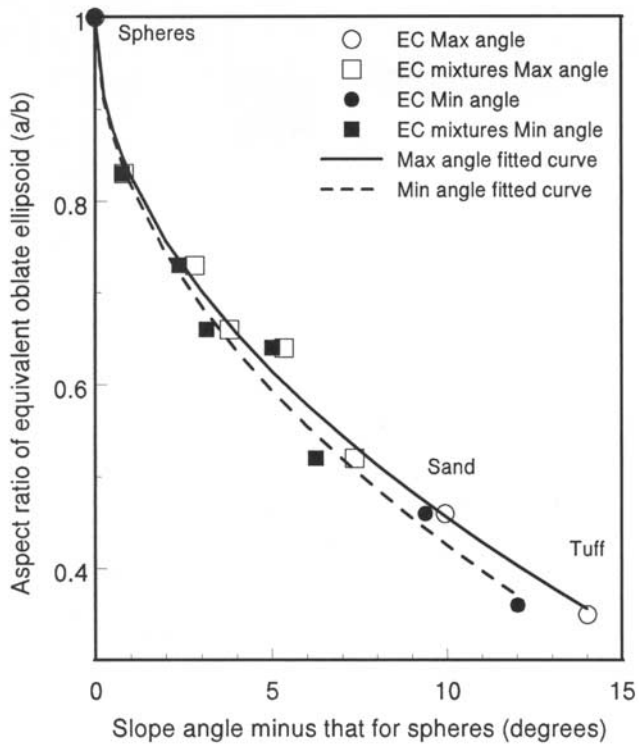

Figure 10. Aspect ratio of equivalent oblate particles best-fitting the $\sigma_a/\sigma_w(\phi)$ measurements as a function of the measured slope angles minus that for spheres.

For nonconducting solid particles ($\sigma_s = 0$) this reduces to:

$$\frac{\sigma_a}{\sigma_w} = \frac{2\phi}{3-\phi} \tag{8b}$$

which seems to serve as an upper bound to the measured $\sigma_a/\sigma_w(\phi)$ relationships (Figure 9), as expected.

[22] A value of 0.2 for the parameter a of the general mixing model (Equation 1) was shown to give the best fit for spheres ($N^{a,b,c}$ = 1/3, 1/3, 1/3). Next, the particle aspect ratios (depolarization factors) were adjusted to fit the $\sigma_a/\sigma_w(\phi)$ measurements of nonspherical particles, giving a/b = 0.460 for the sand grains and a/b = 0.350 for the tuff particles. These aspect ratios (for the sand, tuff and glass-sand mixtures) are plotted as a function of slope angle increase above that for spheres (Figure 10). An empirical function is fitted to the data for the maximum (α_m) and repose (α_r) angles:

$$a/b = \left(\frac{1-(\alpha-\alpha_{sphere})}{\beta}\right)^2 \qquad (r^2 = 0.987) \tag{9}$$

with β = 0.1698 for the maximum angles (r^2 = 0.987) and β = 0.1791 for the repose angles (r^2 = 0.975).

4.5. Prediction of the Dielectric Permittivity Using the Equivalent Oblate Ellipsoid

[23] In an attempt to test the prediction capability of equation 1 (with a = 0.2) and the significance of the aspect ratio of an equivalent oblate particle as a particle shape quantifier, we applied equation 1 to the related but different property of effective permittivity, using a set of dielectric measurements with the same glass spheres, sand grains and tuff grains. The permittivity of the solid, determined using the method outlined by *Robinson and Friedman* [2002b], was 7.6 for glass beads, 4.7 for quartz sand and 6.0 for tuff particles. A value of 0.2 for a was found to best-fit also the dielectric data for glass spheres, indicating on its physical significance, to some extent. Aspect ratios of 0.465 and 0.364 were calculated from the measured maximum angles (Equation 9, β = 0.1698) for the sand and tuff, respectively, and their resemblance to those best-fitted directly to the EC measurements (0.460 and 0.350), indicates on the highly correlated $a/b(\alpha_m)$ relationship (r^2 = 0.987). The predicted effective permittivities, using a = 0.2 and a/b of 1, 0.465 and 0.364, for the glass, sand and tuff, respectively, are presented on Figure 11, showing excellent agreement with the measured data. The Maxwell Garnett (a = 0) prediction defines an upper bound for the measurements with glass spheres. Lines are also presented for the predicted permittivity using a = 0.2, but with the depolarization factors set for spheres ($N^{a,b,c}$ = 1/3, 1/3, 1/3). It is clearly observed that the use of the depolarization factors obtained from the slope measurements greatly improves the prediction, suggesting that the method can be used to account for particle shape from a quantifiable granular property.

[24] Another property affecting the $\sigma_a/\sigma_w(\phi)$ and $\varepsilon_{eff}(\phi)$ relationships of granular materials is the particle size dis-

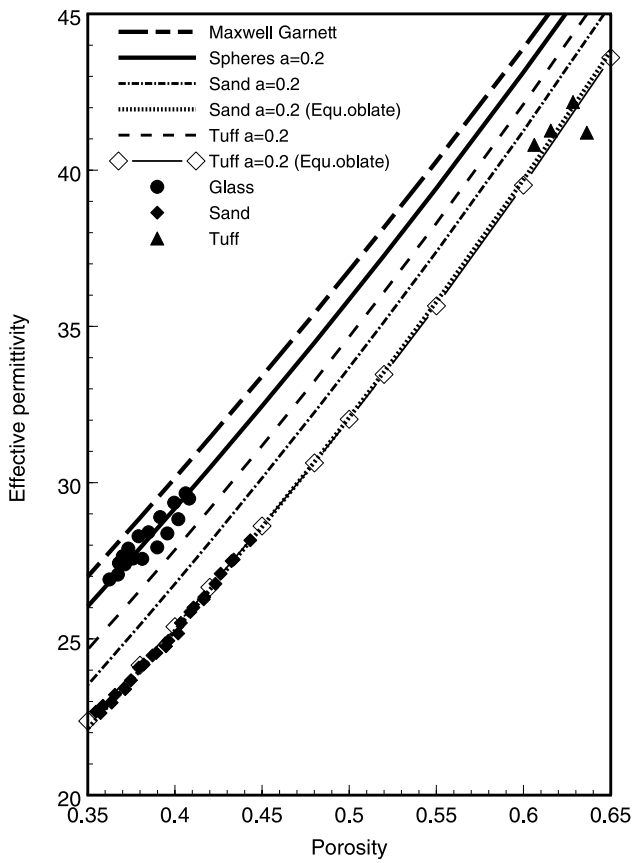

Figure 11. Effective permittivity as a function of porosity for glass beads, quartz sand, and tuff grains. Predictions of permittivity are presented for equivalent oblates of a/b = 0.465 for sand and 0.364 for tuff. Note that the sand and tuff lie on lines close together due to the difference in the permittivity of the solid grains (Table 1).

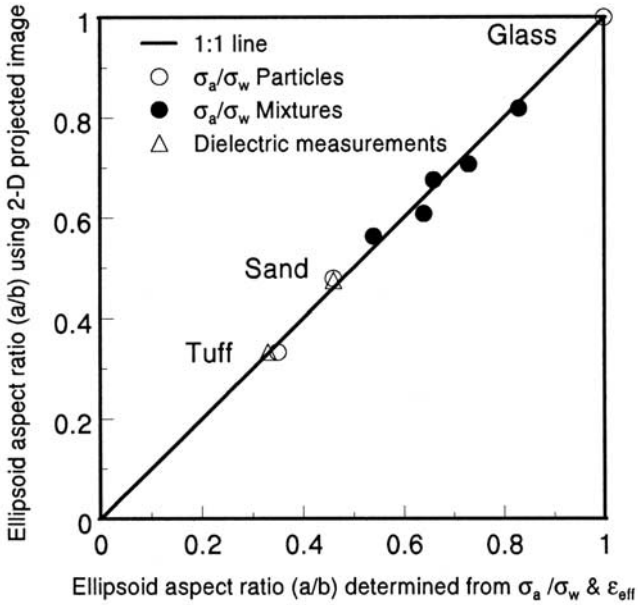

Figure 12. Aspect ratio determined from image analysis of the two-dimensional projections of the particles as a function of the aspect ratios determined by best fitting the general mixing model (equation 1) to measurements of bulk electrical conductivities and effective permittivities.

tribution. Work presented by *Robinson and Friedman* [2001], for example, demonstrated a moderate decrease in the permittivity of water-saturated binary mixtures of glass beads, beyond the expected effect of a decreasing porosity, with a minimum at 1/3 small beads mixed in 2/3 large. Some initial results [*Robinson and Friedman*, 2002a] suggest that slope angles are also affected by the particle size distribution with the maximum angle increasing moderately and the repose angle decreasing moderately compared to mono-sized packings. If this proves to be the case, it would make the maximum angle the more favored of the slope measurements, as it incorporates both particle shape and particle size distribution effects, while maintaining the correct general trend of decreased permittivity with increasing slope angle.

4.6. Prediction of the $\sigma_a/\sigma_w(\phi)$ and $\varepsilon_{eff}(\phi)$ Relationships Using Photographically Determined Aspect Ratios

[25] Particle shape characterization by image analysis of a 2-D projected photograph served in this study only as an intermediate stage in our search for slope angle-particle shape correlations. Although the aspect ratios determined by the image analysis procedure are also in good agreement with those best-fitting the $\sigma_a/\sigma_w(\phi)$ and $\varepsilon_{eff}(\phi)$ measurements via the general mixing model (Figure 12), we do not propose to use image analysis as a routine method. This is because of the problems associated with retrieving the relevant aspect ratios from a plan view in the case of oblate particles (the particle shape assumed in modeling $\sigma_a/\sigma_w(\phi)$ and $\varepsilon_{eff}(\phi)$), and because of the expensive equipment and extensive work involved.

5. Summary and Conclusions

[26] The aspect ratio of an equivalent oblate particle, *a/b*, is a good particle shape quantifier of granular materials for

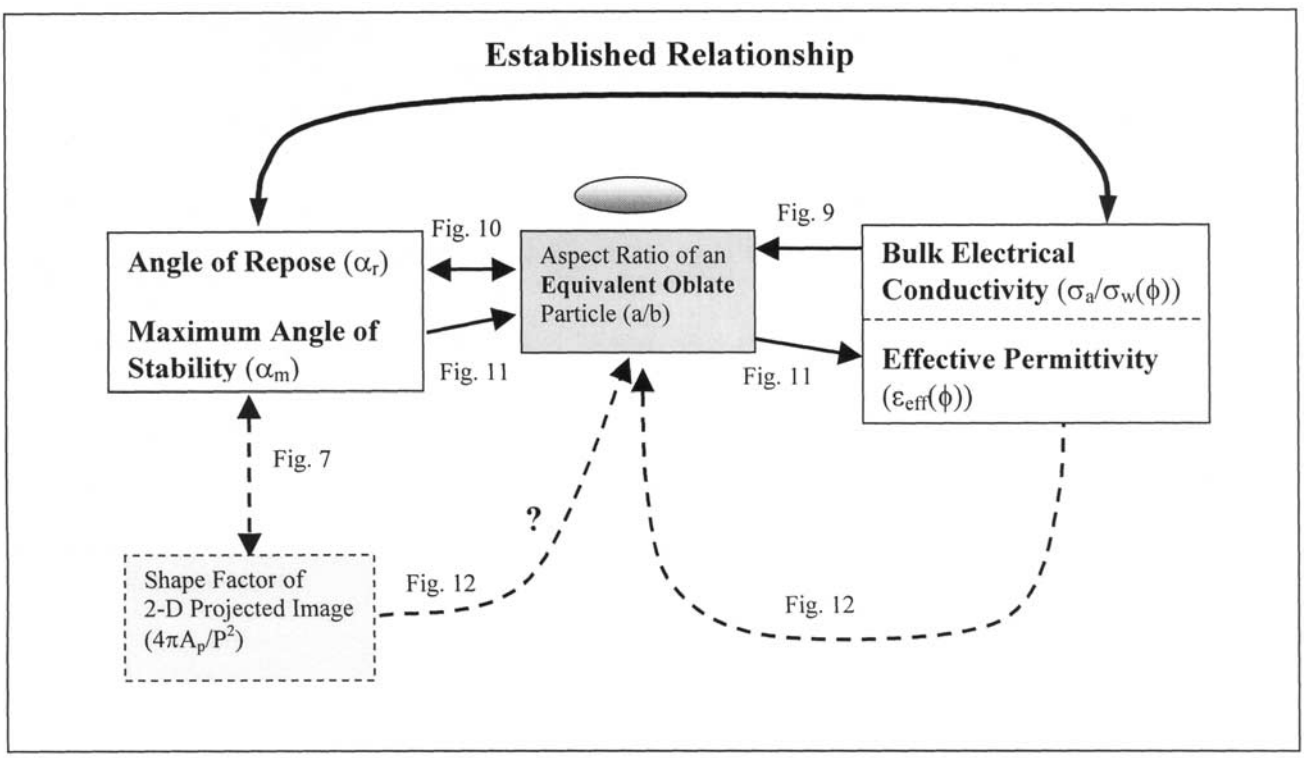

Figure 13. A flowchart describing the relationships tested in this study between slope angles, 2-D projected imaged shape factors, aspect ratios, effective permittivity and bulk electrical conductivity.

the purpose of predicting effective permittivity/electrical conductivity–porosity relationships ($\varepsilon_{eff}(\phi)$, $\sigma_a/\sigma_w(\phi)$). Furthermore, measurements of slope angles (α_m and α_r) are highly correlated with a/b. Therefore slope angle measurements can be used for predicting the $\sigma_a/\sigma_w(\phi)$ and $\varepsilon_{eff}(\phi)$ relationships (and also for characterizing particle shapes for other purposes). The good agreement between the model calculations and the $\sigma_a/\sigma_w(\phi)$ and $\varepsilon_{eff}(\phi)$ measurements also indicates the significance of the value of $a = 0.2$ for the heuristic parameter characterizing the effect of the neighboring particles on the internal electrical field, at least for packings of the kind of materials used in the present study.

[27] The schematic flowchart presented in Figure 13 summarizes the relationships tested in this study. The main proposed route is from slope angles to a/b (of equivalent oblate particle) to $\sigma_a/\sigma_w(\phi)$ and $\varepsilon_{eff}(\phi)$. The unessential bypass through the 2-D projected image analysis is also shown (the question mark denotes the questionable characterizing of an oblate particle shape from a plan view). These initial encouraging findings are based on measurements made with just two types of nonspherical particles and must be substantiated further if the method is to be considered as routine for determining the effective geometry of a granular material. Several questions are opened up, an important one being, which of the slope angles is preferable. From a measurement point of view both angles are easy to measure. For incorporating particle size distribution effects, the maximum angle seems to be preferable. Another important question is how best to determine the slope angle? In this study we used the formation of a slope under water, although suitable for sedimentary materials this may not be suitable for materials such as soils. Future work should determine the applicability of the method to materials such as soils where particle shape is often over looked in the modeling of their dielectric and electrical properties.

[28] **Acknowledgments.** This research was supported by research grant IS-2839-97 from BARD, the United States-Israel Binational Agricultural Research and Development Fund. The authors wish to thank Galit Neves-Piestun and Nirit Bernstein for permitting us and assisting us in using the microscope and camera. Contribution from the Agricultural Research Organization, The Volcani Center, Bet Dagan, Israel, 614/01.

References

Archie, G. E., The electrical resistivity log as an aid in determining some reservoir characteristics, *Trans. AIME*, *146*, 54–62, 1942.

Barabási, A. L., R. Albert, and P. Schiffer, The physics of sand castles: Maximum angle of stability in wet and dry granular media, *Physica A*, *266*, 366–371, 1999.

Brown, D. J., and G. T. Vickers, The use of projected area distribution functions in particle shape measurement, *Powder Technol.*, *98*, 250–257, 1998.

Coelho, D., J. F. Thovert, and P. M. Adler, Geometrical and transport properties of random packings of spheres and aspherical particles, *Phys. Rev. E.*, *55*, 1959–1978, 1997.

Coulomb, C. A., Sur une application des règles de maximis et minimis à quelques problèmes de statique, relatifs à l'architecture, in *Mémoires de Mathématiques et de Physique*, pp. 343–382, Acad. R. des Sci., Paris, 1773.

Dirksen, C., and S. Dasberg, Improved calibration of time domain reflectometry soil water content measurements, *Soil Sci. Soc. Am. J.*, *57*, 660–667, 1993.

Fricke, H., The electric conductivity and capacity of disperse systems, *Physics*, *1*, 106–115, 1931.

Friedman, S. P., and S. B. Jones, Measurement and approximate critical path analysis of the pore scale-induced anisotropy factor of an unsaturated porous medium, *Water Resour. Res.*, *37*, 2929–2942, 2001.

Hallikainen, M. T., F. T. Ulaby, M. C. Dobson, M. A. El-Rayes, and L.-K. Wu, Microwave dielectric behavior of wet soil, part I, Empirical models and experimental observations, *IEEE Trans. Geosci. Remote Sens.*, *GE-23*, 25–34, 1985.

Heimovaara, T. J., Time domain reflectometry in soil science: Theoretical backgrounds, measurements and models, Ph.D. thesis, Univ. of Amsterdam, Amsterdam, 1993.

Heimovaara, T. J., and E. de Water, A computer controlled TDR system for measuring water content and bulk electrical conductivity of soils, *Rep. 41*, Lab. of Phys. Geogr. and Soil Sci., Univ. of Amsterdam, Amsterdam, 1993.

Jaeger, H. M., C.-H. Liu, and S. R. Nagel, Relaxation at the angle of repose, *Phys. Rev. Letters*, *62*, 40–43, 1989.

Jones, S. B., and S. P. Friedman, Particle shape effects on the effective permittivity of anisotropic or isotropic media consisting of aligned or randomly oriented ellipsoidal particles, *Water Resour. Res.*, *36*, 2821–2833, 2000.

Kim, J. H., J. A. Ochoa, and S. Whitaker, Diffusion in anisotropic media, *Transp. Porous Media*, *2*, 327–356, 1987.

Koeppe, J. P., M. Enz, and J. Kakalios, Phase diagram for avalanche stratification of granular media, *Phys. Rev. E.*, *58*, 4104–4107, 1998.

Kraszewski, A. W., *Microwave Aquametry Electromagnetic Wave Interaction With Water-Containing Materials*, edited by A. W. Kraszewski, IEEE Press, Piscataway, N. J., 1996.

Landau, L. D., and E. M. Lifshitz, *Electrodynamics of Continuous Media*, translated by J. B. Sykes and J. S. Bell, Pergamon, New York, 1960.

Maxwell, J. C., *A Treatise on Electricity and Magnetism*, Dover, Mineola, N. Y., 1954.

Maxwell-Garnett, J. C., Colours in metal glasses and in metallic films, *Philos. Trans. R. Soc. London, Ser. A*, *203*, 385–420, 1904.

Mehta, A., *Granular Matter: An Interdisciplinary Approach*, Springer-Verlag, New York, 1994.

Meredith, R. E., and C. W. Tobias, Conduction in heterogeneous systems, *Adv. Electrochem. Electrochem. Eng.*, *2*, 15–47, 1962.

Mualem, Y., and S. P. Friedman, Theoretical prediction of electrical conductivity in saturated and unsaturated soil, *Water Res. Res.*, *27*, 2771–2777, 1991.

Nadler, A., and H. Frenkel, Determination of soil solution electrical conductivity form bulk soil electrical conductivity measurements by four-electrode methods, *Soil Sci. Soc. Am. J.*, *44*, 1216–1221, 1980.

Podczeck, F., A shape factor to assess the shape of particles using image analysis, *Powder Technol.*, *93*, 47–53, 1997.

Polder, D., and J. H. V. van Santen, The effective permeability of mixtures of solids, *Physica*, *12*, 257–271, 1946.

Rhoades, J. D., P. A. C. Ratts, and R. J. Prather, Effects of liquid-phase electrical conductivity, water content, and surface conductivity on bulk soil electrical conductivity, *Soil Sci. Soc. Am. J.*, *40*, 651–655, 1976.

Rhoades, J. D., F. Chanduvi, and S. Lesch, Soil salinity assessment, *FAO Irrig. and Drainage Pap. 57*, Food and Agric. Organ., Rome, Italy, 1999.

Robinson, D. A., and S. P. Friedman, The effect of particle size distribution on the effective dielectric permittivity of saturated granular media, *Water Res. Research*, *37*, 33–40, 2001.

Robinson, D. A., and S. P. Friedman, Observations of the effects of particle shape and particle size distribution on avalanching of granular media, *Physica A*, *311*, 97–110, 2002a.

Robinson, D. A., and S. P. Friedman, A method for measuring the solid particle permittivity or electrical conductivity of rocks, sediments and granular materials, *J. Geophys. Res.*, *107*, doi:10.1029/2001JB000691, in press, 2002b.

Sareni, B., L. Krähenbühl, A. Beroual, and C. Brosseau, Effective dielectric constant of random composite materials, *J. Appl. Phys.*, *81*, 2375–2383, 1997.

Sen, P. N., C. Scala, and M. H. Cohen, A self-similar model for sedimentary rocks with application to the dielectric constant of fused glass beads, *Geophysics*, *46*, 781–795, 1981.

Sihvola, A., *Electromagnetic Mixing Formulas and Applications*, *IEE Electromagnetic Waves Ser.*, vol. 47., Inst. of Electrical Eng., Stevenage, UK, 1999.

Sihvola, A., and J. A. Kong, Effective permittivity of dielectric mixtures, *IEEE Trans. Geosci. Remote Sens.*, *26*, 420–429, 1988.

Sperry, J. M., and J. J. Peirce, A model for estimating the hydraulic conductivity of granular material based on grain shape, grain size and porosity, *Ground Water*, *33*, 892–898, 1995.

Topp, G. C., J. L. Davies, and A. P. Annan, Electromagnetic determination of soil water content: Measurements in coaxial transmission lines, *Water Resour. Res.*, *16*, 574–582, 1980.

Torquato, S., Thermal conductivity of disordered heterogeneous media from the microstructure, *Rev. Chem. Eng.*, *4*, 151–204, 1987.

Tsang, L., J. A. Kong, and R. T. Shin, *Theory of Microwave Remote Sensing*, John Wiley, New York, 1985.

Vickers, G. T., The projected areas of ellipsoids and cylinders, *Powder Technol.*, *86*, 195–200, 1996.

Vickers, G. T., and J. Brown, The distribution of projected area and perimeter of convex, solid particles, *Proc. R. Soc. London, Ser. A*, *457*, 283–306, 2001.

Wardell, H., Volume, shape and roundness of quartz particles, *J. Geol.*, *43*, 250–280, 1935.

Wyllie, M. R. J., and A. R. Gregory, Formation factors of unconsolidated porous media: Influence of particle shape and effect of cementation, *Petrol. Trans. AIME*, *198*, 103–109, 1953.

Wyllie, M. R. J., and A. R. Gregory, Fluid flow through unconsolidated porous aggregates: Effect of porosity and particle shape on Kozeny-Carman constants, *Indust. Eng. Chem.*, *47*, 1379–1388, 1955.

Yong, R. N., and B. P. Warkentin, *Soil Properties and Behaviour*, *Dev. Geotech. Eng.*, vol. 5, Elsevier Sci., New York, 1975.

Zimmerman, R. W., Effective conductivity of a two-dimensional medium containing elliptical inhomogeneities, *Proc. R. Soc. London, Ser. A*, *47*, 1713–1727, 1996.

S. P. Friedman, Institute of Soil, Water and Environmental Sciences, Agricultural Research Organization, Bet Dagan 50250, Israel. (vwsfried@agri.gov.il)

D. A. Robinson, U.S. Salinity Laboratory, 450 West Big Springs Road, Riverside, CA 92507, USA.